

Simultaneous Measurement of Refractive Index and Thickness with a Convergent Beam

King Ung Hui^{1,2*} and Kuan Hiang KWEK¹

¹Department of Physics, Faculty of Science, University of Malaya, 50603 Kuala Lumpur, Malaysia

²Faculty of Engineering, Computing and Science, Swinburne University of Technology, Sarawak Campus, 93350 Kuching, Malaysia

(Received March 31, 2014; Revised July 2, 2014; Accepted July 2, 2014)

A new approach to the simultaneous measurement of refractive index and thickness based on the focus shifts of a convergent beam intercepted by a test plate is proposed. By using ray optics, a defined focus shift can be derived as a function of the refractive index and thickness as well as the angular position of the test plate with respect to the optical axis. From a pair of focus shifts obtained at two different angular positions, it is shown that the desired measurands can be simultaneously determined without prior knowledge of either parameter. A simulation result for the proposed concept based on graphically solving the equations of their respective focus shifts is presented.

© 2014 The Japan Society of Applied Physics

Keywords: optical measurements and metrology, refractive index, thickness, optical materials, geometrical optics

1. Introduction

The characterization of optical materials that involves the measurements of their refractive index n and thickness d is increasingly essential in various research fields and applications. For a plane-parallel transparent plate, the determination of refractive index requires knowledge of the thickness and vice versa. In the literature, various optical methods have been developed to determine both measurands simultaneously without prior knowledge of either parameter.^{1–13}

In general, these techniques are essentially based on either the translational scanning on a test plate with a focusing beam that converts the measurands n and d into a displacement measure,^{1–5} or the rotational scanning of a test plate in a parallel beam that induces a beam displacement or an equivalent optical path change according to the parameters n and d .^{6–10} Other optical methods that require no mechanical translation or rotation during the measurement process have also been reported.^{11–13} However, these methods require the use of a light source with a certain wavelength range as well as the processing or measurement algorithm of the interference signals.

In this paper, we theoretically show the method for the simultaneous measurement of refractive index and thickness based on the focus shifts induced when a test plate is inserted into a convergent beam and oriented at different angular positions with respect to the optical axis. The focus shift is defined and geometrically derived as a function of refractive index, thickness, and angular position. In this method, the convergent beam is transmitted through the test plate to induce focus shift, and therefore the use of a monochromatic light source is sufficient. Furthermore, no rotational scanning over a certain angular range or signal processing algorithm is required. The proposed method is verified through a simulation experiment with solving graphically the equa-

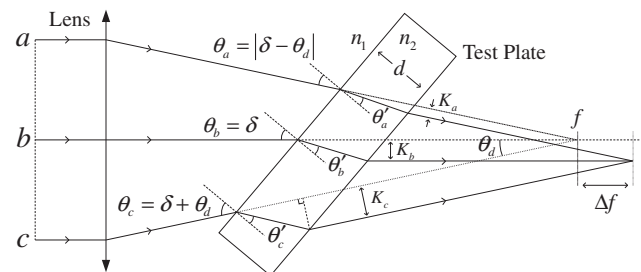


Fig. 1. Illustration of the longitudinal component of focus shift, Δf induced by a test plate placed at angular position δ in a convergent beam.

tions of various focus shifts to determine simultaneously the refractive index and thickness of a test plate.

2. Theoretical Basis

In Fig. 1, a convergent beam is prepared by focusing a nominally plane wavefront with a good collimating lens that converges rays into a focus at f without inserting a test plate. Upon the insertion of a test plate into the path of the convergent beam and in an orientation perpendicular to the optical axis ($\delta = 0$ deg), the focus shifts longitudinally along the optical axis due to the refractions in the test plate. With its dependence on the same parameters of the plate, the magnitude of the focus shift can be increased when the angular position δ of the test plate is increased from its minimum. In this case, on top of the longitudinal shift induced, there is also a lateral shift of the focus from the optical axis as shown in Fig. 1. However, in the proposed method of simultaneous measurement, only the longitudinal component of the shift, Δf , (Fig. 1) needs to be considered, and this is used to define the measure of the focus shift.

The magnitude of focus shift can be geometrically derived by tracing the three main rays, ray- a , ray- b , and ray- c according to Snell's law. From Fig. 1, the incident angle θ_b for ray- b is directly the angular position δ of the test plate,

*E-mail address: khii@swinburne.edu.my

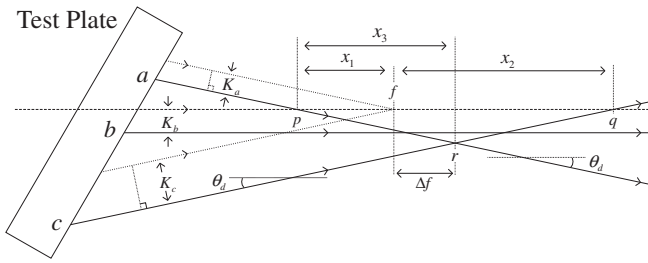


Fig. 2. Detailed view of the focus shift as defined by the circle of least confusion formed at point r .

which is set to zero when the plate is normal to the optical axis. The incident angles for the ray- a and ray- c are $\theta_a = |\delta - \theta_d|$ and $\theta_c = \delta + \theta_d$, respectively, where θ_d is the half-divergence angle of the convergent beam. The value of θ_d is approximated to $\sin \theta_d \approx \tan \theta_d$ for paraxial ray tracing.

In general, upon refractions on both parallel surfaces of the test plate, a ray shifts sideways parallel to its propagation direction by a factor K as shown in Fig. 1. The factor K can be expressed as $K = dI$, where d is the thickness of the test plate and I is the angular factor which is a function of the incident angle θ_i and the refractive indices of air (n_1) and the test plate (n_2). I is derived (Appendix) to be

$$I = \sin \theta_i \left(1 - \frac{n_1 \cos \theta_i}{\sqrt{n_2^2 - n_1^2 \sin^2 \theta_i}} \right). \quad (1)$$

At normal position, both ray- a and ray- c are incident on the test plate at the same incident angle θ_d , yielding the same amount of shift of $K_a = K_c$ that displaces the focus longitudinally along the optical axis. However, when departing from the normal position, all the rays shift proportionally to their angle of incidence at different magnitudes of K . Hence, these rays cross each other at different points rather than coincide into a focus outside the optical axis as shown in Fig. 2.

For derivation purpose, an isosceles triangle of pqr with $pr = qr$ is outlined (Fig. 2). Points p and q are the respective intersections of ray- a and ray- c with the optical axis, while point r is the intersection between ray- a and ray- c . In this case, the focus shift Δf is defined and derived as the longitudinal component between the focus point f and point r (Fig. 2). In practice, the position of point r can be experimentally traced since it is the position of the circle of least confusion.

Geometrically, $\Delta f = x_3 - x_1$ where $x_3 = (x_1 + x_2)/2$ since both ray- a and ray- c are inclined to the principal axis at the same angle of θ_d . From $x_1 = K_a/\sin \theta_d$ and $x_2 = K_c/\sin \theta_d$, Δf becomes

$$\Delta f = \frac{K_c - K_a}{2 \sin \theta_d} = \frac{d(I_c - I_a)}{2 \sin \theta_d}, \quad (2)$$

where the term $I_c - I_a$ is derived (Appendix) as

$$I_c - I_a = 2 \sin \theta_d \cos \delta - \frac{\frac{1}{2} n_1 \sin[2(\delta + \theta_d)]}{\sqrt{n_2^2 - n_1^2 \sin^2(\delta + \theta_d)}}$$

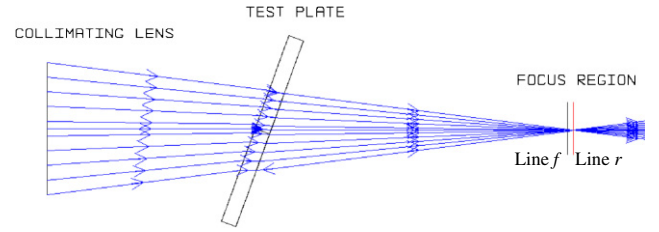


Fig. 3. (Color online) Layout of ZEMAX simulation showing the longitudinal shift of the focus from the position of line f (without insertion of test plate) to line r for a test plate placed at an arbitrary angular position.

$$+ \frac{\frac{1}{2} n_1 \sin[2(\delta - \theta_d)]}{\sqrt{n_2^2 - n_1^2 \sin^2(\delta - \theta_d)}}. \quad (3)$$

According to Eq. (2), the unknown d can be eliminated by taking the ratio of two focus shifts obtained at different angular positions, and the measurand of n can therefore be determined. In this work, an approach to graphing Eq. (2) for different focus shifts over a series of inferred d and n values is employed. The intersection of the plots therefore indicates the correct n and d values of the test plate used. In principle, any plot of other combinations of focus shifts obtained from the same test plate should satisfy the same intersection (see discussion in the next section).

3. Simulation Experiment

For verification, a simulation experiment using a commercial ray-tracing program (ZEMAX) is performed to obtain the focus shifts induced by a test plate inserted in a convergent beam as shown in Fig. 3. In a paraxial mode, a collimating lens with a focal length of $f = 100.00$ mm is used to converge a beam with a diameter of $\phi = 5.00$ mm. The half-divergence angle is given by $\theta_d = \tan^{-1}(\phi/2f)$. The light source of helium-neon laser (wavelength of 632.8 nm) is used, and the air refractive index is set to unity.

The position of the initial focus obtained without inserting a test plate is first marked and recorded. Subsequently, a test plate of N-BK7 with an arbitrary thickness of 2955.00 μm and a refractive index of 1.51509 (at a wavelength of 632.8 nm) is inserted into the convergent beam. Upon plate insertion, the new position of the shifted focus is marked and measured with respect to the position of the initial focus point. Next, the test plate is rotated to various angular positions starting from the normal position. The corresponding focus shifts induced are recorded accordingly as shown in Table 1. In this case, the focus shift is measured at an accuracy of $\pm 1 \times 10^{-3} \mu\text{m}$ while the angular position of the test plate is set with an accuracy of $\pm 1 \times 10^{-6}$ deg.

From the data obtained, the plots of d versus n according to Eq. (2) for the corresponding focus shifts and their angular positions are obtained as shown in Fig. 4. The single intersection of all plots indicates the correct n and d values of the test plate used, which are found to be 1.51509 and 2955.00 μm , respectively. The achievement of the single intersection in this case indicates high measurement

Table 1. Focus shifts measured at various angular positions.

Angular position δ (deg)	Focus shift $\Delta f \pm 0.001 \mu\text{m}$
0	1004.965
10	1040.204
20	1148.592
30	1337.088
40	1612.681

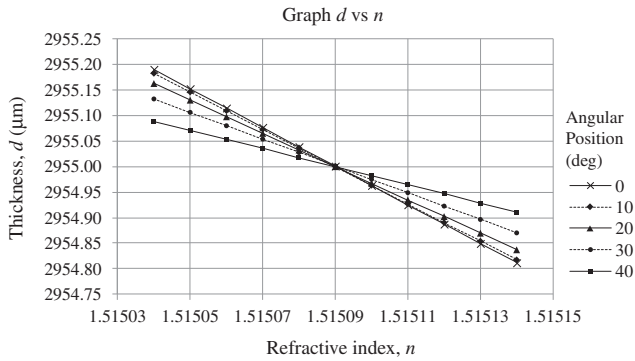


Fig. 4. Plot of d versus n of Eq. (2) for various focus shifts over series of inferred d and n values. The correct n and d values are simultaneously shown by the intersection.

accuracies of n and d . However, these accuracies are considerably nominal as the simulation is carried out in a paraxial mode as well as with high accuracies in angular positioning and focus shift measurement applied. For example, the accuracies of the axes of both n and d as shown in Fig. 4 can be, in fact, increased beyond the real practical limit as all perfect plots satisfy the same intersection. Incidentally, the factor of θ_d is derived from the focal length and beam diameter used, on which the accuracy of θ_d depends. However, since these parameters (f , ϕ , and θ_d) are taken to be constant, their accuracies are therefore not involved in the estimation of the measurement accuracies of n and d .

In practice, the experimental verification of the proposed method has been performed by using a half-aperture four-field lateral shearing interferometer for focus shift measurement.¹⁴ The interferometer utilized the approach of collimation detection in tracing the focus shifts, which can be performed at an estimated accuracy of $\pm 2 \mu\text{m}$. The accuracy of angular positioning is ± 0.05 deg while the constant of θ_d is derived from $f = 100$ mm and $\phi = 5$ mm. The refractive index of air is taken to be unity. Accounting for the uncertainties of measurements, a refractive index in the third decimal place and a thickness accurate to within an average of $\pm 6 \mu\text{m}$ were experimentally determined for the measurements of the BK7 and fused silica samples.¹⁴ These measurement accuracies are comparable to the ones obtained by Refs. 5, 7, and 10. The proposed method of simultaneous measurement can be employed with various detection techniques for focus shift as long as high accuracies can be achieved. For an improved detection technique for the

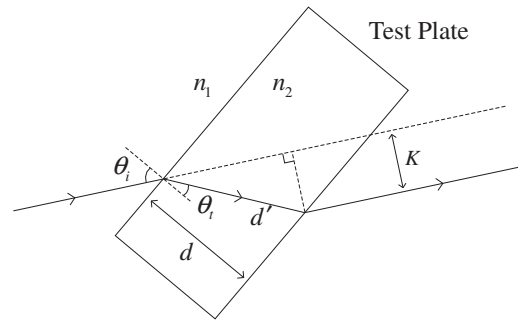


Fig. A-1. Factor K (lateral shift) of a ray incident at an angle on a parallel plate.

focus shift used, the accuracies of the simultaneous measurement based on the proposed method would be improved accordingly.

4. Conclusions

The principle of the simultaneous measurement of refractive index and thickness based on focus shift measurements is discussed. Simulation result shows that with at least two focus shifts obtained at different angular positions, the measurands n and d can be determined without prior knowledge of either parameter. The proposed method could be applied with other systems or techniques that could accurately measure the defined focus shift. The method has been verified experimentally.

Acknowledgements

This work was supported by the University of Malaya Short-Term Research Grant (PS124/2007B) and the MOSTI Research Grant (06-01-03-SF0296).

Appendix

From Fig. A-1, the thickness d and lateral shift K can be geometrically derived as

$$d = d' \cos \theta_t, \quad (\text{A}\cdot 1)$$

$$K = d' \sin(\theta_i - \theta_t), \quad (\text{A}\cdot 2)$$

respectively.

Dividing Eq. (A-2) by Eq. (A-1) gives

$$K = d \frac{\sin(\theta_i - \theta_t)}{\cos \theta_t}. \quad (\text{A}\cdot 3)$$

Here, the angular factor is defined as

$$I = \frac{\sin(\theta_i - \theta_t)}{\cos \theta_t}. \quad (\text{A}\cdot 4)$$

Expanding Eq. (A-4) gives

$$I = \sin \theta_i - \cos \theta_i \tan \theta_t. \quad (\text{A}\cdot 5)$$

According to Snell's law,

$$\sin \theta_t = \frac{n_1 \sin \theta_i}{n_2}. \quad (\text{A}\cdot 6)$$

From Eq. (A-6), $\tan \theta_t$ can be trigonometrically determined as

$$\tan \theta_i = \frac{n_1 \sin \theta_i}{\sqrt{n_2^2 - n_1^2 \sin^2 \theta_i}}. \quad (\text{A}\cdot 7)$$

Substituting Eq. (A·7) into Eq. (A·5) yields

$$I = \sin \theta_i \left(1 - \frac{n_1 \cos \theta_i}{\sqrt{n_2^2 - n_1^2 \sin^2 \theta_i}} \right). \quad (\text{A}\cdot 8)$$

Substitutions of $\theta_c = \delta + \theta_d$ and $\theta_a = \delta - \theta_d$ for I_c and I_a , respective, give

$$\begin{aligned} I_c - I_a &= \sin(\delta + \theta_d) - \sin(\delta - \theta_d) \\ &\quad - \frac{n_1 \sin(\delta + \theta_d) \cos(\delta + \theta_d)}{\sqrt{n_2^2 - n_1^2 \sin^2(\delta + \theta_d)}} \\ &\quad + \frac{n_1 \sin(\delta - \theta_d) \cos(\delta - \theta_d)}{\sqrt{n_2^2 - n_1^2 \sin^2(\delta - \theta_d)}}. \end{aligned} \quad (\text{A}\cdot 9)$$

Furthermore, Eq. (A·9) can be trigonometrically simplified as

$$\begin{aligned} I_c - I_a &= 2 \sin \theta_d \cos \delta - \frac{\frac{1}{2} n_1 \sin[2(\delta + \theta_d)]}{\sqrt{n_2^2 - n_1^2 \sin^2(\delta + \theta_d)}} \\ &\quad + \frac{\frac{1}{2} n_1 \sin[2(\delta - \theta_d)]}{\sqrt{n_2^2 - n_1^2 \sin^2(\delta - \theta_d)}}. \end{aligned} \quad (\text{A}\cdot 10)$$

References

- 1) H. Maruyama, T. Mitsuyama, M. Ohmi, and M. Haruna: *Opt. Rev.* **7** (2000) 468.
- 2) I. K. Ilev, R. W. Waynant, K. R. Byrnes, and J. J. Anders: *Opt. Lett.* **27** (2002) 1693.
- 3) M. Ohmi, H. Nishi, Y. Konishi, Y. Yamada, and M. Haruna: *Meas. Sci. Technol.* **15** (2004) 1531.
- 4) S. Kim, J. Na, M. J. Kim, and B. H. Lee: *Opt. Express* **16** (2008) 5516.
- 5) Y. P. Kumar and S. Chatterjee: *Appl. Opt.* **51** (2012) 3533.
- 6) G. Coppola, P. Ferraro, M. Iodice, and S. D. Nicola: *Appl. Opt.* **42** (2003) 3882.
- 7) G. D. Gillen and S. Guha: *Appl. Opt.* **44** (2005) 344.
- 8) R. Ince and E. Huseyinoglu: *Appl. Opt.* **46** (2007) 3498.
- 9) H. J. Choi, H. H. Lim, H. S. Moon, T. B. Eom, J. J. Ju, and M. Cha: *Opt. Express* **18** (2010) 9429.
- 10) B. Hussain, M. Ahmed, M. Nawaz, M. Saleem, M. Razzaq, M. A. Zia, and M. Iqbal: *Appl. Opt.* **51** (2012) 5326.
- 11) J. Jin, J. W. Kim, C.-S. Kang, J.-A. Kim, and T. B. Eom: *Opt. Express* **18** (2010) 18339.
- 12) S. J. Park, K. S. Park, Y. H. Kim, and B. H. Lee: *IEEE Photonics Technol. Lett.* **23** (2011) 1076.
- 13) J. Park, L. Chen, Q. Wang, and U. Griesmann: *Opt. Express* **20** (2012) 20078.
- 14) K. U. Hii: MSc. Thesis, Faculty of Science, University of Malaya, Kuala Lumpur (2011).